

X-rays, clumping and wind structures

Lidia Oskinova^{1*}, Wolf-Rainer Hamann¹, Richard Ignace², and Achim Feldmeier¹

¹ Universität Potsdam, Germany

² East Tennessee State University, TN, USA

Abstract: X-ray emission is ubiquitous among massive stars. In the last decade, X-ray observations revolutionized our perception of stellar winds but opened a Pandora's box of urgent problems. X-rays penetrating stellar winds suffer mainly continuum absorption, which greatly simplifies the radiative transfer treatment. The small and large scale structures in stellar winds must be accounted for to understand the X-ray emission from massive stars. The analysis of X-ray spectral lines can help to infer the parameters of wind clumping, which is prerequisite for obtaining empirically correct stellar mass-loss rates. The imprint of large scale structures, such as CIRs and equatorial disks, on the X-ray emission is predicted, and new observations are testing theoretical expectations. The X-ray emission from magnetic stars proves to be more diverse than anticipated from the direct application of the magnetically-confined wind model. Many outstanding questions about X-rays from massive stars will be answered when the models and the observations advance.

1 Introduction

Two aspects in studies of X-ray emission from massive stars attract most attention: *i*) how X-rays are generated in massive stars, and *ii*) how X-ray emission can be used in analyzing stellar winds. In the basic concept, the wind has two components: a general cool wind with temperature of $T_w \sim 10$ kK which contains nearly all the wind mass, and a hot tenuous component with $T_X \sim \text{few MK}$ where the X-rays originate. The X-ray photons suffer continuum K-shell absorption in the cool wind and, in turn, can affect the wind ionization via the Auger process.

In this review we concentrate on X-ray emission from single stars. This is thermal emission from gases heated in the stellar wind shocks or in magnetically confined wind regions. Cassinelli & Olson (1979) proposed X-radiation from a base coronal zone plus Auger ionization in the surrounding cool wind to explain the superionization (e.g. N V, O VI) that was observed to be present in Copernicus UV spectra of OB stars. From the analysis of *Einstein* spectra of OB-stars, Cassinelli & Swank (1983) concluded that the base corona idea was not correct since soft X-rays were observed. The Si XIII and S XV line emission was detected in the SSS spectrum of the O-star ζ Ori. These ions correspond to high temperature and are located at a energy where the wind would be thin to X-rays. This led to a conclusion about two sources of X-ray emission, X-rays that arise from fragmented shocks in the wind and X-rays from very hot, probably magnetically confined loops, near the base of the wind. Furthermore since X-ray variability was already known to be less than about 1%, Cassinelli

*lida@astro.physik.uni-potsdam.de

& Swank (1983) suggested that there had to be thousands of shock fragments in the wind. Radiation hydrodynamic simulations of the nonlinear evolution of instabilities in stellar winds were performed by Owocki, Castor, & Rybicki (1988). They demonstrated that the X-ray can originate from plasma heated by strong reverse shocks, which arise when a high-speed, rarefied flow impacts on slower material that has been compressed into dense shells. Feldmeier, Puls, & Pauldrach (1997) assumed a turbulent seed perturbation at the base of the stellar wind and found that the shocks arising when the shells collide are capable of explaining the observed X-ray flux. These 1D hydrodynamical models predict plasma with temperatures 1–10 MK which is permeated with the cool wind. X-rays suffer absorption as they propagate outwards through the ensemble of dense, radially compressed shells.

Waldron (1984) calculated the opacity of O-star winds for the X-ray radiation. The absorption of X-rays in Wolf-Rayet (WR) star winds was investigated by Baum et al. (1992). They employed detailed non-LTE stellar atmosphere models and showed that since the WR wind opacity is very high, the observed X-rays must emerge from the far outer wind region. Hillier et al. (1993) computed the wind opacity of the O5Ia star ζ Pup. They found that the high opacity of the stellar wind would completely block the soft X-rays (< 0.5 keV) unless some significant fraction of hot plasma is located far out in the wind, at distances exceeding $100 R_*$.

The shape of X-ray emission line profiles was predicted by MacFarlane et al. (1991). They considered the effect of wind absorption on the emission from an expanding shell of hot gas. When the cool wind absorption is small, the line is broad and has a box-like shape. For stronger wind absorption, the line becomes more skewed (see Fig. 7 in MacFarlane et al. 1991). The line shape is largely determined by a parameter τ_0 :

$$\tau_0 = \kappa_\lambda R_* = \rho_w \chi_\lambda R_* \quad (1)$$

where R_* [cm] is the stellar radius, and the atomic opacity κ_λ is the product of the mass absorption coefficient χ_λ [$\text{cm}^2 \text{g}^{-1}$] and the density of the cool wind (ρ_w) as defined from the continuity equation $\dot{M} = 4\pi\rho_w v(r)r^2 R_*^2$, where r is the radial distance in units of R_* , and $v(r)$ is the velocity law, that can be prescribed by the formula $v(r) = v_\infty(1 - 1/r)^\beta$. MacFarlane et al. notice that when τ_0 increases, the red-shifted part of the line ($\Delta\lambda > 0$) becomes significantly more attenuated than the blue-shifted part. They suggested that evaluating the line shape can be used to determine τ_0 . The K-shell opacity varies with wavelength with the power between 2 and 3 (Hillier et al. 1993), therefore in the X-ray band τ_0 should change by orders of magnitude. Consequently, the X-ray emission line shape at shorter and longer wavelengths should be different. Waldron & Cassinelli (2001) expanded the single-shock model of MacFarlane et al. and considered emission from spherically symmetric shocks equally distributed between $0.4v_\infty$ and $0.97v_\infty$ with temperatures ranging from 2 to 10 MK. In similar spirit, Ignace (2001) provided a formalism that accounts for the emission from a flow that is embedded with zones of X-ray emitting gas. Owocki & Cohen (2001) calculated model X-ray line profiles for various combinations of the parameters β , τ_0 , and onset radii for X-ray emission.

2 The high-resolution X-ray spectra of O-type supergiants

Waldron & Cassinelli (2001) obtained the first high-resolution X-ray spectrum of an O star. Their analysis of this *Chandra* spectrum of the O9.7Ib star ζ Ori revealed that the hot plasma is located relatively close to the stellar core and that the line profiles appear to be symmetric, and not skewed.

Subsequent analyses of X-ray spectra of single O-type stars are broadly consistent with these first results. The *XMM-Newton* RGS spectra of two O-type stars are shown in Fig. 1. The general properties of X-ray emission from massive stars are summarized in Waldron & Cassinelli (2007) and Güdel & Nazé (2009) (see also Nazé 2011, these proc.). The X-ray spectra of O-stars are well described by a thermal plasma with temperatures spanning between $\approx 2 - 10$ MK. The ratio between

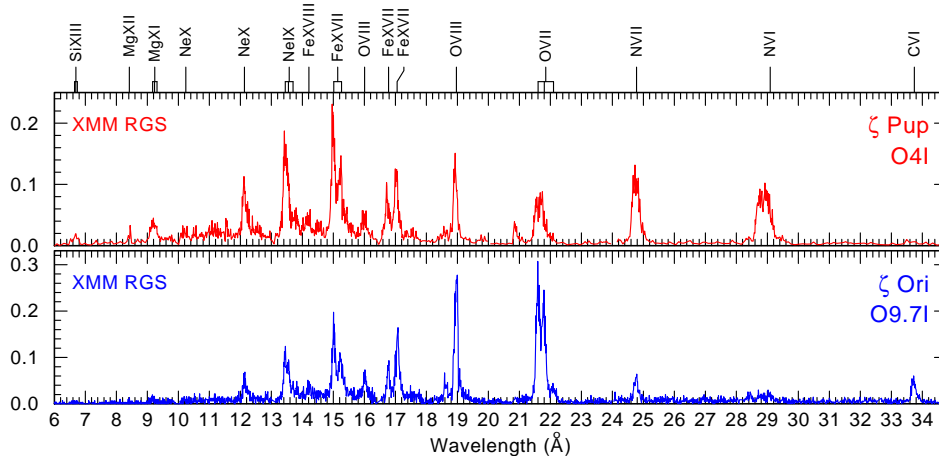


Figure 1: RGS spectrum of the O4Ief star ζ Pup (top panel) and of the O9.7Ib star ζ Ori (bottom panel), not corrected for interstellar absorption. The ζ Pup spectrum results from the combination of separate exposures accumulating about 530 ks of useful exposure time. In the case of ζ Pup, the strength of the nitrogen lines compared to the oxygen and carbon lines clearly indicates an overabundance of nitrogen.

the fluxes in forbidden and intercombination lines of He-like ions indicates that the line formation region lies between $\approx 1.2 - 20 R_*$ (e.g. Leutenegger et al. 2006). The line widths are proportional to the terminal wind speed as obtained from UV line diagnostics. The values of τ_0 (see Eq. 1) are small and the emission line profiles are similar across the X-ray spectrum.

3 How to reconcile theory and observations

The high-resolution X-ray spectra present two key problems. First, how to explain the origin of X-rays at a distance of a few tens of stellar radii from the photosphere? Second, how to explain the shape of the X-ray emission lines and their similarity across the spectrum?

The presence of magnetic fields may help to heat the plasma very close to the stellar surface (e.g. Cassinelli & Olson 1979). Recently, this idea was boosted by the direct measurement of magnetic fields on some massive stars (e.g. Bouret et al. 2008a). Waldron & Cassinelli (2007) pointed out a “high-ion near star problem”: the radii of formation for the lines of ions with higher ionization potential ions are closer to the surface than those of lower ions. Their proposed explanation invokes magnetic fields. Unfortunately, the signal-to-noise ratio in the lines of He-like ions of Si, S, Ar, and Ca, which provide the diagnostics for the hottest plasma, is rather low. Better quality data are needed to pin-point the exact location of the hot plasma in massive star winds in order to verify the claim of Waldron & Cassinelli.

However, surface magnetic fields may not be required to explain the available measurements. The simulations of instabilities in stellar winds (Runacres & Owocki 2002, 2005) show that strong shocks may develop at the distances which agree well with those inferred from the analysis of He-like ions.

Below, we briefly consider some solutions proposed to explain the observed emission line profiles:

- i*) Line optical depth alters the line shape of X-ray emission profiles (Ignace & Gayley 2002);
- ii*) Reduction of the wind absorption column density implying a lower \dot{M} (e.g. Waldron & Cassinelli 2001; Cassinelli et al. 2001; Kramer, Cohen, & Owocki 2003);
- iii*) Macroclumping resulting in smaller effective opacity (e.g. Feldmeier, Oskinova, Hamann 2003; Oskinova, Feldmeier, Hamann 2006; Owocki & Cohen 2006; Cassinelli et al. 2008).

3.1 Optically thick X-ray emitting plasma

Ignace & Gayley (2002) calculated X-ray line profiles produced in an hot plasma that is optically thick. They found that the optically thick lines have nearly symmetrical shape. Leutenegger et al. (2007) used this formalism to show that the resonance lines of He-like ions of N and O in the X-ray spectrum of ζ Pup are better described under the assumption of resonant scattering.

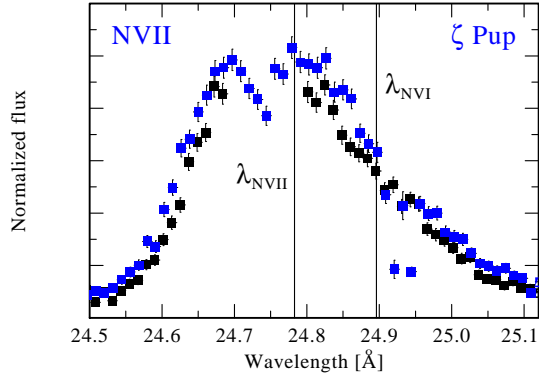


Figure 2: The N VII λ 24.758 and N VI λ 24.898 blend in the *XMM-Newton* RGS1 (blue line) and RGS2 (red line) spectra of ζ Pup. The central wavelengths of corresponding lines are indicated.

Further evidence that some X-ray lines can be optically thick comes from the characteristic shapes, e.g. the dip at the top of the N VII line in ζ Pup spectrum (Fig. 2). Such line structures are typical for optically thick emission lines in the optical spectra of WR stars, e.g. He II λ 5412 Å in WR3. As estimated by Ignace & Gayley (2002), the X-ray lines of leading ions in the most dense winds can indeed be optically thick. However, the lines of less abundant ions (such as S, Si, Ne, Fe) originating in the less dense winds cannot be explained by resonant scattering.

3.2 Reducing the wind absorption column density

The observed X-ray emission lines in O-star spectra are typically symmetrical and similar across the X-ray spectrum. Fitting observed lines with MacFarlane et al. line model, generally yields low values of τ_0 and its weak dependence on wavelength (e.g. Cassinelli et al. 2001, Kahn et al. 2001, Miller et al. 2002, Kramer et al. 2003, Pollock 2007). Recalling that $\tau_0 \propto \kappa_\lambda = \chi_\lambda \rho_w$, these empiric results can be explained by the weak wavelength dependence of opacity and by the reduced wind density ρ_w .

The wind opacity for the X-rays is mainly due to K-shell ionization of metals. In O-stars κ_λ chiefly depends on the chemical composition, but little on other details of the wind models (Oskinova et al. 2006). Hence, knowing the metal abundances is prerequisite to calculate wind opacity.

The abundance in O-type stars are often non-solar (e.g. Lamers et al. 1999). Example of typical ON-type star with enhanced nitrogen abundance is ζ Pup. Using non-LTE wind atmospheres, Pauldrach, Hoffmann, & Lennon (2001) found that while N is overabundant in this star, C and O are depleted. They show that the N/C ratio is 20×solar and the N/O ratio is 10×solar in ζ Pup. Fig. 3 demonstrates our model fit to the UV spectrum of ζ Pup, assuming abundances as derived in Pauldrach et al.. The lines of C, N, and O are well reproduced.

The abundances obtained from the analysis of X-ray spectra of ζ Pup are in general agreement with those from Pauldrach et al. (e.g. Fig. 1, also Kahn et al. 2001). Leutenegger et al. (2007) estimate that nitrogen has twice the abundance of oxygen in ζ Pup. Krtićka & Kubàt (2007) show that the use of new 3D solar abundances (Asplund et al. 2005) with lower metallicity improves the agreement between observation and wind theory. Their calculations of κ_λ in ξ Per agree well with those in Oskinova et al. (2006).

At softer X-ray energies the large wind optical depth for the X-rays is largely determined by the CNO edges (see Fig. 20 in Pauldrach et al.). Selectively reduced metal abundance would lead to a drop in the jump heights in wind opacity due to the edges, leading to less pronounced wavelength dependence of optical depth. Recently, Cohen et al. (2010) assumed that in ζ Pup the abundance ratio of N/C is $60\times$ solar and N/O is $25\times$ solar, which resulted in the less steep jumps of wind optical depths at the wavelengths of the K-shell edges. They claimed that this wind optical depth agrees with the marginal wavelength dependence of τ_0 (on 68% confidence limits) which they found by fitting the lines in the *Chandra* spectrum of ζ Pup. For consistency, we calculated the H α line adopting the same wind parameters as used by Cohen et al. (2010) for their X-ray line model. The resulting model H α line shows a large discrepancy with the observed one. This points out that the parameters used by Cohen et al. to model the X-ray lines may not be realistic.

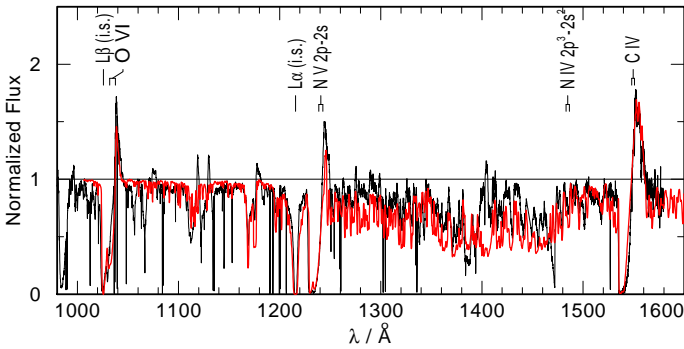


Figure 3: The EUV spectrum of ζ Pup, observed with FUSE (black line), compared to a PoWR model spectrum (red line). The resonance doublets of C IV, N V and O VI are well reproduced, as well as the forest of iron-group lines. The O VI doublet can only be fitted with models accounting for a diffuse X-ray field. (Adopted from Oskinova et al. 2006).

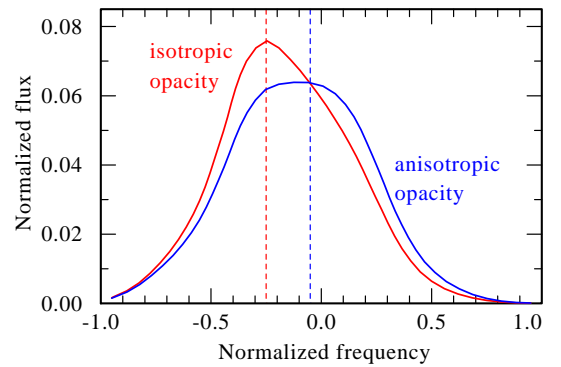


Figure 4: Two model lines calculated using the same wind parameters but assuming isotropic and anisotropic clumps. Isotropic opacity leads to a significantly more skewed line.

The observed nearly symmetric shapes of the X-ray emission lines can be explained if the wind density, ρ_w , is small. The reduction of the density can be expected from atmosphere models that account for wind *clumping*.

The inhomogeneity of stellar winds has been established in the last decade (see reviews in Hamann et al. 2008). The mass-loss rates are empirically inferred from modeling recombination and resonance lines in the optical and UV. The recombination line strength depends on ρ_w^2 , while the resonance line strength depends on ρ_w . Assuming that the interclump medium is void and that the density within the clumps is enhanced by a factor D , the \dot{M} inferred from analysis of recombination lines has to be reduced by factor $\sqrt{D^{-1}}$ compared to the values obtained under the assumption of a smooth wind.

Assuming that nearly all mass is in clumps, the volume filling factor is $f_V \approx D^{-1}$. In order to fit recombination and resonant lines simultaneously, the wind models require very small filling factors (Fullerton, Massa, & Prinja 2006). Consequently, these models require a reduction of empirically inferred \dot{M} up to a factor of 100 compared to the unclumped models.

Waldron & Cassinelli (2010) proposed an alternative solution to the problem of the mass-loss rate discordance. They pointed out that the XUV radiation near the He II ionization edge originating in wind shocks would destroy P V ions. Consequently, the key diagnostic resonant line of P V would be weakened and could be explained without the need to decrease \dot{M} . The source of the XUV radiation could be the bow-shocks around the wind clumps as proposed in Cassinelli et al. (2008).

The models with severely reduced mass-loss rates encounter substantial problems when one tries to explain the observed X-ray line spectra:

- i) The low values of \dot{M} do not explain why the shapes of X-ray lines show no significant wavelength dependence.
- ii) Eq. 1 can be used to model the X-ray lines only assuming that the clumps are optically thin. This strong assumption (often referred to as *microclumping* approximation) is not always valid.

4 Macroclumping

4.1 On the size of optically thick clumps

There is no known reason why the microclumping approximation should apply. The optical depth of an isotropic clump (i.e. with the same dimensions in 3D) is

$$\tau_{\text{clump}}(\lambda) = \rho_w \chi_\lambda D d_{\text{clump}} R_* = \frac{\dot{M} \chi_\lambda}{4\pi v_\infty R_*} \cdot \frac{d_{\text{clump}}}{f_V} \cdot \frac{1}{(1 - \frac{1}{r})^\beta r^2} \equiv \tau_*(\lambda) \frac{d_{\text{clump}}}{f_V} \cdot \frac{1}{(1 - \frac{1}{r})^\beta r^2}, \quad (2)$$

where d_{clump} is the geometrical size of the clump expressed in R_* . The strong wavelength dependence of χ_λ suggests that a clump may be optically thick at long wavelengths but thin at short ones.

It is convenient to express $\tau_*(\lambda)$ as

$$\tau_*(\lambda) \approx 722 \frac{\dot{M}_{-6}}{v_\infty \mathcal{R}_*} \cdot \chi_\lambda, \quad (3)$$

where \dot{M}_{-6} is the mass-loss rate in units $10^{-6} M_\odot \text{ yr}^{-1}$, v_∞ is the terminal velocity in $[\text{km s}^{-1}]$, and $\mathcal{R}_* = R_*/R_\odot$. If at some radius r , the clump size is larger than $d_{\text{clump}}^{\tau=1}$, such clump is not optically thin for the X-ray radiation at λ . The size of a clump with optical depth $\tau = 1$ at wavelength λ is

$$d_{\text{clump}}^{\tau=1} = \frac{f_V}{\tau_*(\lambda)} \cdot \left(1 - \frac{1}{r}\right)^\beta r^2. \quad (4)$$

The microclumping approximation is valid only for significantly smaller clumps.

It is a common misconception to assume that *macroclumping*, which allows for any clump optical depth, implies a geometrically large size of clumps. Let us estimate the geometrical size of a clump which has optical depth unity. We consider ζ Pup and use parameters from Zsargo et al. (2008): $\dot{M}_{-6} = 1.7$, $v_\infty = 2300$, $\mathcal{R} = 19$, $\beta = 0.9$. Thus, $\tau_*(\lambda) \approx 0.03 \chi_\lambda$. Then a clump with optical depth unity has the size

$$d_{\text{clump}}^{\tau=1}(\zeta \text{ Pup}) = \frac{f_V}{0.03} \cdot \frac{1}{\chi_\lambda} \cdot \left(1 - \frac{1}{r}\right)^{0.9} r^2. \quad (5)$$

For a sample of O-stars, Bouret et al. (2008b) find $0.01 < f_\infty < 0.08$, where f_∞ is the filling factor in wind regions where $v_w = v_\infty$ (see Bouret et al. for details). For a rough estimate we adopt $f_V = 0.03$. Then a clump of optical depth unity has the size $d_{\text{clump}}^{\tau=1}(\zeta \text{ Pup}) = \chi_\lambda^{-1} \cdot (1 - \frac{1}{r})^{0.9} r^2$. Zsargo et al. (2008) do not provide χ_λ values, and we are not aware of any consistent calculation χ_λ for the low values of \dot{M} . Adopting $\dot{M}_{-6} = 4.2$, Oskinova et al. (2006) derive $\chi_\lambda \approx 60 [\text{cm}^2 \text{ g}^{-1}]$ at 12\AA and $\chi_\lambda \approx 180 [\text{cm}^2 \text{ g}^{-1}]$ at 19\AA . To roughly account for the lower mass-loss rate, we reduce these values by a factor of two. The geometrical sizes of clumps which have optical depth unity at 12\AA and 19\AA in ζ Pup wind are shown in Table 1. Note that if \dot{M} is higher, clumps with even smaller geometrical sizes will be optically thick.

Table 1: Estimate of the geometrical size of a clump with optical depth unity at wavelength λ in the wind of ζ Pup. The wind parameters are from Zsargo et al. (2008) $M_{-6} = 1.7$, $v_\infty = 2300$, $R = 19$, $\beta = 0.9$. Compared to Oskinova et al. (2006), χ_λ is scaled down by a factor of two to account for the smaller \dot{M} adopted in Zsargo et al. (2008).

Wavelength λ	χ_λ [cm ² g ⁻¹]	$d_{\text{clump}}(\tau_\lambda = 1) [R_*]$	
		At $R = 2R_*$ in the wind	At $R = 5R_*$ in the wind
12	30	0.07	0.7
19	90	0.02	0.2

It is possible that the clumps in ζ Pup wind have sizes similar to shown in Table 1, and, thus, are optically thick at the corresponding wavelengths. Therefore the X-ray line profile fitting based on the microclumping approximation can lead to the erroneous results.

4.2 Effective opacity

The idea that clumping may reduce the wind opacity and lead to more symmetric line profiles was briefly discussed in Waldron & Cassinelli (2001), Owocki & Cohen (2001) and Kramer et al. (2003). The effects of wind clumping on the X-ray lines were investigated in detail in Feldmeier et al. (2003), who solved the pure absorption case of radiative transfer in clumped winds and found that the emission lines are more symmetric than in the case of a smooth wind. In Oskinova et al. (2006) we employed a 2.5-D Monte-Carlo code (Oskinova et al. 2004) to compute the emission line profile for a finite number of clumps and compared the results to the observed lines.

The effective opacity, κ_{eff} , in a clumped wind is the product of:

- average number of clumps per unit volume, $n(r)$ [cm⁻³]
- geometrical cross-section of a clump, σ_{clump} [cm²]
- probability that an X-ray photon with a wavelength λ which encounters a wind clump gets absorbed, $\mathcal{P} = 1 - e^{-\tau_{\text{clump}}(\lambda)}$

Thus,

$$\kappa_{\text{eff}} = n(r) \cdot \sigma_{\text{clump}} \cdot \mathcal{P} = \frac{\rho_w \chi_\lambda}{\tau_{\text{clump}}} \cdot (1 - e^{-\tau_{\text{clump}}(\lambda)}), \quad (6)$$

where we used Eq. (2) and expressed the filling factor as $f_V = D^{-1} = n(r)V_{\text{clump}}$ with $V_{\text{clump}} = \sigma_{\text{clump}}d_{\text{clump}}R_*$. In the case of optically thin clumps ($\tau_{\text{clump}} \ll 1$) the effective opacity is $\kappa_{\text{eff}} = n(r) \cdot \sigma_{\text{clump}} \cdot \tau_{\text{clump}} = \rho_w \chi_\lambda \equiv \kappa_\lambda$, recovering the microclumping approximation. In the case of optically thick clumps ($\tau_{\text{clump}} \gg 1$), the absorption probability is $\mathcal{P} = 1$, yielding $\kappa_{\text{eff}} = n(r)\sigma_{\text{clump}}$. In this limit of porous wind, the opacity does not depend of the wavelength, but is “gray”.

In general, the effective opacity is wavelength dependent. As can be seen from Eqs. (2) and (6), the dependence on wavelength enters via the clump optical depth: $\kappa_{\text{eff}} \propto 1 - e^{-\tau_{\text{clump}}(\lambda)}$. This reduced dependence of effective opacity on wavelength agrees well with observations.

Evaluating the wind optical depth as an integral over effective opacity along the line-of-sight z :

$$\tau_w = \int_{z_\nu}^{\infty} n(r)\sigma_{\text{clump}}(1 - e^{-\tau_\nu^{\text{clump}}})dz, \quad (7)$$

where z is the coordinate along the line of sight. Motivated by the results of the hydrodynamic simulations which predict radially compressed wind structures, Feldmeier et al. (2003) studied the case

of radially compressed clumps, with $\sigma_{\text{clump}} \propto |dr/dz|$. In this case, the integral in Eq. (7) transforms into an integral over r . As a result, the X-ray emission line profiles will be nearly symmetric (see Fig. 4), while in the case of isotropic clumps the line profiles are more skewed (see also Hervé & Rauw 2011, these proc.). Hence, lower values of τ_0 are obtained when the X-ray lines are fitted using the specific assumption of spherical clumps compared to the case of angular dependent opacity.

4.3 The impact of clumping on empirical mass-loss rate estimates

Owocki, Gayley, & Shaviv (2004) studied the effects of porosity on the atmospheres of LBV stars. Massa et al. (2003) and Fullerton et al. (2006) discussed how porosity can affect the formation of P Cygni lines. Prinja & Massa (2010) found the spectroscopic signatures of wind clumping, and show that macroclumping must be taken into account to model the UV resonance lines. The effect of macroclumping on *line opacity* was studied for the first time in Oskinova, Hamann, & Feldmeier (2007). The macroclumping was incorporated in the state-of-the-art non-LTE atmosphere model PoWR (e.g. Gräfener, Koesterke & Hamann 2002). We have shown that accounting for clumps leads to empirical mass-loss rate estimates which are by a factor of a few higher than those obtained under the assumption of microclumping, but are still reduced compared to a smooth wind.

In the case of line opacity, an additional parameter, v_D is required, which describes the velocity field *within* the clump. The detailed UV line fits for O stars require a "microturbulence velocity" of 50 to 100 km s⁻¹, which, perhaps, can be attributed to the velocity dispersion within clumps. Figures 5 and 6 illustrate the effect of macroclumping on resonance lines. With a lower velocity dispersion within a clump, the Doppler broadening becomes smaller, and the line absorption profile is narrower but peaks higher. Thus, the clump optical depth becomes larger in the line core, but smaller in the line wings. In the statistical average, this leads to a reduction of the effective opacity and a weakening of the line (see also Sundqvist et al. 2011, these proc.).

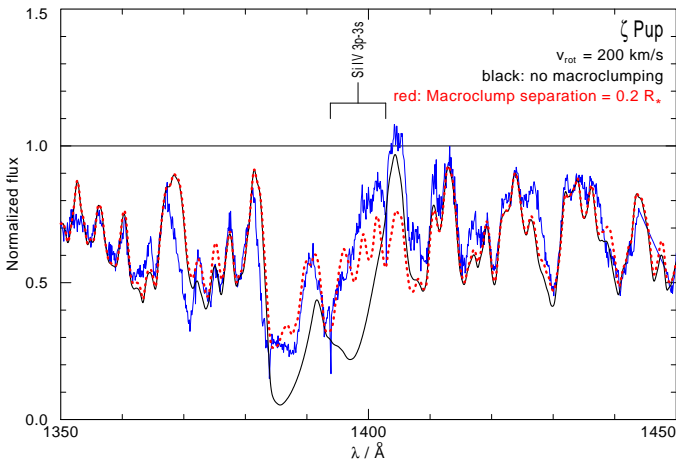


Figure 5: Effect of macroclumping on the Si IV doublet. The IUE spectrum of ζ Pup is shown in blue. The usual microclumping modeling yields P Cygni features that are too strong (black, continuous line). With our macroclumping formalism, the line features are reduced to the observed strength (red, dotted curve).

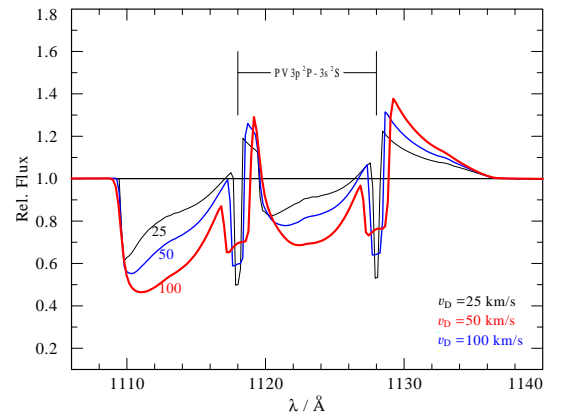


Figure 6: Synthetic P V resonance doublet at λ 1118/1128 Å for different values of the microturbulence velocity v_D (labels). All other model parameters are kept fixed. When the velocity dispersion across the clumps is decreased, the macroclumping effect becomes more pronounced and leads to a weaker line profile.

At present macroclumping is included in the non-LTE model atmosphere only as a first approximation. Even though the results are very encouraging because consistent mass-loss rates can be

obtained simultaneously from the analysis of UV, optical, and X-ray spectra. As an example, our analyses of H α , P V, and Si IV lines and the X-ray emission lines all agree with a value for the mass-loss rate of $\dot{M} \approx 2.5 \times 10^{-6} M_{\odot} \text{ yr}^{-1}$ in the wind of ζ Pup (Oskinova et al., in prep.).

5 The large scale structures in stellar winds and the X-rays

5.1 X-rays and Co-rotating Interaction Regions

In the previous section, we discussed the small-scale, stochastic wind inhomogeneities. Beside those, there is strong evidence for the presence of large-scale structures in stellar winds. Spectral lines formed in stellar winds are variable, e.g. discrete absorption components (DACs) are observed in the UV resonance lines of nearly all O stars (Prinja & Howarth, 1986). Cranmer & Owocki (1996) explained DACs as originating from co-rotating interaction regions (CIR), where high-density, low-speed streams collide with low-density, high-speed streams. The observed slow drift of DACs can be understood by considering the motion of the patterns in which the DAC features are formed (Hamann et al. 2001). The hydrodynamics of stellar winds which can explain the DACs and the faster modulations are considered by Lobel et al. (2011, these proc.).

This complex wind geometry should affect the production and the propagation of X-rays in stellar winds: the wind can be shocked at the CIR surfaces (Mullan 1984). X-rays may suffer additional absorption in density enhanced CIRs.

The DACs recurrence time is on time scale of days. Oskinova, Clarke, & Pollock (2001) detected periodic X-ray variability with an amplitude of $\sim 20\%$ in the ASCA passband (0.5-10 keV) of the O9Ve star ζ Oph. The detected period of 0^d.77 possibly indicates a connection with the recurrence time (0^d.875 \pm 0^d.167) of the DACs in the UV spectra of this star. In contrast, the analysis of 1^d.175 continuous ASCA observations of ζ Pup failed to confirm the previously reported variability at the 6% level with a period of 16.667 h found in earlier Rosat data. The new, more sensitive analyses of X-ray observations of O-stars which will extend over the stellar rotational periods should shed more light on the connections between DACs, rotation, and X-ray emission.

5.2 X-ray emission from Oe-type stars

ζ Oph belongs to the rare class of Oe stars (Negueruela, Steele, & Bernabeu 2004). Oe-type stars display Balmer lines similar to those in the classical Be stars. The latter are fast rotating stars with decretion disks. Negueruela et al. point out that the Oe-phenomenon is restricted to the latest subtypes among the O stars, indicating that the building of disks is more problematic for the higher-mass stars.

Li et al. (2008) studied the X-ray emission from Oe/Be stars to test whether the disks of these stars could form by magnetic channeling of wind toward the equator (Cassinelli et al. 2002). In their model, X-rays can be produced by material that enters the shocks above and below the disk region. The model by Li et al. predicts an existence of a relation between L_X/L_{bol} and the magnetic field strength in Oe/Be stars.

High-resolution X-ray spectra are only available for two Oe stars: ζ Oph (O9Ve) and HD 155806 (O7.5Ve). The X-ray properties of these stars are quite different. ζ Oph shows periodic modulations of the X-ray flux, has narrow X-ray emission lines. The bulk of its plasma is at a high temperature of 8 MK (Zhekov & Palla 2004). Nazé et al. (2010a) do not detect a modulation of the X-ray flux in HD 155806 and report that its X-ray emission lines are broad. The bulk of its hot plasma has only 2 MK. The $\log L_X/L_{\text{bol}} = -6.75$ for HD 155806, while $\log L_X/L_{\text{bol}} = -7.4$ for ζ Oph (Oskinova et al. 2006, Nazé et al. 2010a). Clearly, larger observational samples are required to understand the link between the X-ray emission of Oe-type stars and their hypothetical circumstellar disks.

5.3 X-ray emission from O-stars with magnetic fields

Large-scale flow structures in stellar winds can result when a large-scale magnetic field confines the outflow of matter. Babel & Montmerle (1997) studied the case of a rotating star with a sufficiently strong dipole magnetic field. Collision between the wind components from the two hemispheres in the closed magnetosphere leads to a strong shock and X-ray emission. Based on this magnetically confined wind shock model (MCWS), the presence of a magnetic field on the O-type star θ^1 Ori C had been postulated. Direct confirmation of the magnetic field in this star by Donati et al. (2002) proved that X-rays have large diagnostic potential in selecting massive stars with surface magnetic fields.

The MHD simulations in the framework of the MCWS model were performed by ud-Doula & Owocki (2002) and Gagné et al. (2005). Using as input parameters the characteristic values of the wind and the magnetic field strength of θ^1 Ori C, these simulations predict the plasma temperature, emission measure, and periodic X-ray flux modulation which compare well with observations.

This modeling success established the MCWS model as a general scenario for the X-ray emission from magnetic early type stars. The MCWS model makes predictions that can be directly compared with observations: *i*) the hottest plasma should be located at a few stellar radii from the stellar surface at the locus where the wind streams collide; *ii*) the X-ray emission lines should be rather narrow, because the hot plasma is nearly stationary; *iii*) magnetic stars should be more X-ray luminous than their non-magnetic counterparts of similar spectral type; *iv*) the X-ray spectrum of magnetic stars should be harder than that of non-magnetic stars, with the bulk of the hot plasma at temperatures ~ 20 MK; *v*) the X-ray emission should be modulated periodically as a consequence of the occultation of the hot plasma by a cool torus of matter, or by the opaque stellar core. X-ray variability may be expected when the torus breaks up.

The X-ray observation of magnetic O-type stars led to perplexing results that are not always in agreement with the model predictions. ζ Ori A has a weak surface magnetic field, that may be responsible for the presence of hot plasma close to stellar surface (Waldron & Cassinelli 2007). But, in general, its X-ray properties are typical for an O-type star (Raassen et al. 2008). A strong magnetic field (~ 1 kG) is detected on HD 108 (O7I) (Martins et al. 2010). However, the emission measure (EM) of the softer spectral component, with a temperature of ≈ 2 MK, is more than one order of magnitude higher than the EM of the harder component $T_{\max} \approx 15$ MK, contrary to the expectation of the MCWS model (Nazé et al. 2004). HD 191612 also has a ~ 1 kG strong magnetic field (Donati et al. 2006a). Recently, Nazé et al. (2010b) demonstrated that the large EM at ≈ 2 MK and the broad X-ray emission lines in the X-ray spectrum of this star do not compare well with the predictions of the MCWS model. The early-type B-star τ Sco has a complex magnetic field topology (Donati et al. 2006b) and a hard X-ray spectrum (Wojdowski & Schulz 2002, Mewe et al. 2003). A substantial modulation of the X-ray flux with stellar rotation period was expected, but indications for only marginal variability were found by Ignace et al. (2010).

Overall, considering the analysis of X-ray observations of magnetic O stars, it appears that only one star, θ^1 Ori C, displays the properties that are fully compatible with the MCWS model.

5.4 X-ray emission from WR stars

The X-ray emission from WR-type stars remains enigmatic – some WN-type stars are X-ray sources (Ignace et al. 2003, Skinner et al. 2010), while others remain undetected despite low upper limits on L_X (Gosset et al. 2005). Oskinova et al. (2003) showed that WC-type stars are not X-ray sources, a result which they attribute to the very large wind opacity. WO-type star winds are even more metal enriched. However, a reduction in the mass-loss (a poorly constrained parameter) by a factor of only two and/or a higher effective stellar temperature result in a higher degree of wind ionization. In this case a fraction of X-rays could escape. Wind anisotropy can further mitigate wind attenuation.

Magnetic fields and large-scale distortions of stellar winds are invoked as possible explanations for the recently detected X-ray emission from the WO-type star WR 142 (Oskinova et al. 2009). WR 142 is a massive star in a very advanced evolutionary stage shortly before its explosion as a supernova or γ -ray burst. From qualitative considerations we conclude that the observed X-ray radiation is too hard to allow wind-shock origin of X-ray emission. The proposed explanation of its X-ray emission suggests surface magnetic field. Possibly related, WR 142 seems to rotate extremely fast, as indicated by the unusually round profiles of its optical emission lines. Our X-ray detection implies that the wind of WR 142 must be relatively transparent to X-rays, which could be due to strong wind ionization, wind clumping, or non-spherical geometry from rapid rotation.

6 Open questions

We find that incorporating macroclumping in the wind models allows to explain the shapes of X-ray emission lines in O-star spectra. However, many questions about X-rays from single massive stars remain. We list a subjective selection of these questions, which we think are the most promising ones to answer with new advances in theory and observations:

- Is there a correlation between T_X and T_{eff} as found by Walborn, Nichols, & Waldron (2009)?
- Is there a near star high ion problem? Is there a dependence of τ_0 on the radius of line formation?
- What is the origin of the $L_X \propto L_{\text{bol}}$ correlation and how to explain deviations from it?
- Does the MCWS model explains the different X-ray properties of magnetic OB-stars?
- Why X-rays from Oe/Be stars are not meeting the model expectations?
- How X-rays are produced in WR-stars?

Acknowledgements

Authors are grateful to J. P. Cassinelli for the insightful discussion.

References

- Asplund, M., Grevesse, N., & Sauval, A.J. 2005, ASP Conf. Ser., 336, 25
- Babel, J., & Montmerle, T. 1997, A&A, 323, 121
- Baum, E., Hamann, W.-R., Koesterke, L., Wessolowski, U., 1992, A&A, 266, 402
- Bouret, J.-C., Donati, J.-F., Martins, F., et al., 2008a, MNRAS, 389, 75
- Bouret, J.-C., Lanz, T., Hillier, D., et al., 2008b, Clumping in Hot Star Winds, Universitätsverlag, Potsdam, p.31
- Cassinelli, J.P. & Olson, G.L., 1979, ApJ 229, 304
- Cassinelli, J.P. & Swank, J.H., 1983, 271, 681
- Cassinelli, J.P., Miller, N.A., Waldron, W.L., MacFarlane, J.J., Cohen, D.H. et al., 2001, ApJ, 554, 55
- Cassinelli, J.P., Brown, J.C., Maheswaran, M., Miller, N.A., Telfer, D.C., 2002, ApJ, 578, 951
- Cassinelli, J.P., Ignace, R., Waldron, W.L., Cho, J., Murphy, N.A., Lazarian, A. 2008, ApJ, 683, 1052
- Cohen, D., Leutenegger, M. A., Wollman, E.E., et al. 2010, MNRAS, 405, 2391
- Cranmer, S.R. & Owocki, S.P., 1996, ApJ, 462, 469
- Donati, J.-F., Babel, J., Harries, T. J., et al., 2002, MNRAS, 333, 55
- Donati, J.-F., Howarth, I. D., Bouret, J.-C., Petit, P., Catala, C., Landstreet, J., et al., 2006a, MNRAS, 365, L6
- Donati, J.-F., Howarth, I.D.; Jardine, M.M., et al., 2006b, MNRAS, 370, 629
- Gagné, M., Oksala, M.E., Cohen, D.H. et al. 2005, ApJ, 628, 986
- Gosset, E., Nazé, Y., Claeskens, J.-F., Rauw, G., Vreux, J.-M., Sana, H. 2005, A&A, 429, 685
- Güdel, M. & Nazé, Y., 2009, A&ARv, 17, 309
- Gräfener, G., Koesterke, L., & Hamann, W.-R., 2002, A&A, 387, 244

Feldmeier, A., Puls, J., Pauldrach, A. W. A., 1997, *A&A*, 320, 899
Feldmeier, A., Oskinova, L., Hamann, W.-R., 2003, *A&A*, 403, 217
Fullerton, A. W., Massa, D. L., & Prinja, R. K. 2006, *ApJ*, 637, 1025
Hamann, W.-R., Brown, J.C., Feldmeier, A., Oskinova, L.M. 2001, *A&A*, 378, 946
Hamann, W.-R. et al., 2008, *Clumping in Hot Star Winds*. Universitätsverlag, Potsdam
Hervé, A. & Rauw, G., 2011, *LIAC2010*
Hillier, D. J., Kudritzki, R.P., Pauldrach, A.W., et al., 1993, *A&A*, 276, 117
Ignace, R., 2001, *ApJ*, 549, 119
Ignace, R., Oskinova, L. M., & Brown, J. C., 2003, *A&A*, 408, 353
Ignace, R. & Gayley, K. G., 2002, *ApJ*, 568, 954
Ignace, R., Oskinova, L. M., Jardine, M. et al., 2010, *ApJ*, 721, 1412
Kahn, S.M., Leutenegger, M. A., Cottam, J., et al. 2001, *A&A*, 365, 312
Kramer, R.H., Cohen, D.H., Owocki, S.P., 2003, *ApJ* 592, 532
Krtička, J. & Kubát, J., 2007, *A&A*, 464, 17
Lamers, H.J.G.L.M., Haser, S., de Koter, A., Leitherer, C., 1999, *ApJ*, 516, 872
Leutenegger, M.A., Paerels, F.B.S, Kahn, S.M., Cohen, D.H., 2006, *ApJ*, 650, 1096
Leutenegger, M.A., Owocki, S.P., Kahn, S.M., & Paerels, F.B.S. 2007, *ApJ*, 659, 642
Li, Q., Cassinelli, J.P., Brown, J.C., Waldron, W.L., Miller, N.A., 2008, *ApJ*, 672, 1174
Lobel, A. et al., 2011, *LIAC2010*
MacFarlane, J.J., Cassinelli, J.P., Welsh, B.Y., Vedder, P.W., Vallerger, J. V., Waldron, W. L. 1991, *ApJ* 380, 564
Martins, F., Donati, J.-F., Marcolino, W.L.F., et al., 2010, *MNRAS*, 407, 1423
Massa, D. Fullerton, A.W., Sonneborn, G., Hutchings, J. B., 2003, *ApJ*, 586, 996
Mewe, R., Raassen, A.J.J., Cassinelli, J.P., van der Hucht, K. A., Miller, N. A., Güdel, M., 2003, *A&A*, 398, 203
Miller, N.A., Cassinelli, J.P., Waldron, W.L., MacFarlane, J.J., Cohen, D.H., 2002, *ApJ*, 577, 951
Mullan, D.J., 1984, *ApJ* 283, 303
Nazé, Y.; Rauw, G.; Vreux, J.-M.; De Becker, M. 2004, *A&A*, 417, 667
Nazé, Y., 2011, *LIAC2010*
Nazé, Y.; Rauw, G.; Ud-Doula, A., 2010a, *A&A*, 510, 59
Nazé, Y., ud-Doula, A., Spano, M., Rauw, G., De Becker, M., Walborn, N.R., 2010b, *A&A*, 520, 59
Negueruela, I., Steele, I.A., Bernabeu, G., 2004, *AN*, 325, 749
Oskinova, L.M., Clarke, D., Pollock, A.M.T., 2001, *A&A*, 378, L21
Oskinova, L.M., Ignace, R., Hamann, W.-R., Pollock, A.M.T., Brown, J.C., 2003, *A&A*, 402, 755
Oskinova, L.M., Feldmeier, A., Hamann, W.-R., 2004, *A&A*, 422, 675
Oskinova, L.M.; Feldmeier, A.; Hamann, W.-R., 2006, *MNRAS*, 372, 313
Oskinova, L.M., Hamann, W.-R., Feldmeier, A., 2007, *A&A*, 476, 1331
Oskinova, L.M, Hamann, W.-R., Feldmeier, A., Ignace, R., Chu, Y.-H., 2009, *ApJL*, 693, 44
Owocki, S. P., Castor, J. I., Rybicki, G. B., 1988, *ApJ*, 335, 914
Owocki, S.P. & Cohen, D. H., 2001, *ApJ*, 559, 1108
Owocki, S.P., Gayley, K.G., Shaviv, N.J., 2004, *ApJ*, 616, 525
Owocki, S.P. & Cohen, D. H., 2006, *ApJ*, 648, 565
Pauldrach, A.W.A, Hoffmann, T.L, Lennon, M., 2001, *A&A* 375, 161
Pollock, A. M. T., 2007, *A&A*, 463, 1111
Prinja, R.K. & Howarth, I.D., 1986, *ApJS*, 61, 357
Prinja, R.K & Massa, D., 2010, *A&A*, 521, L55
Raassen, A.J.J., van der Hucht, K.A., Miller, N.A., Cassinelli, J.P., 2008, *A&A*, 478, 513
Runacres, M. C. & Owocki, S. P., 2002, *A&A*, 381, 1015
Runacres, M. C. & Owocki, S. P., 2005, *A&A*, 429, 323
Skinner, S.L., Zhekov, S.A., Güdel, M., Schmutz, W., Sokal, K.R., 2010, *AJ*, 139, 825
Sundqvist, J., et al., 2011, *LIAC2010*
Walborn, N.R., Nichols, J. S., Waldron, W.L., 2009, *ApJ*, 703, 633
Waldron, W. L., 1984, *ApJ*, 282, 256
Waldron, W. L. & Cassinelli, J. P., 2001, *ApJ*, 548, 45
Waldron, W. L. & Cassinelli, J. P., 2007, *ApJ*, 668, 456
Waldron, W. L. & Cassinelli, J. P., 2010, *ApJ*, 711, 30
Wojdowski, P.S & Schulz, N.S, 2002, *ApJ*, 627, 953
ud-Doula, A., & Owocki, S. P. 2002, *ApJ*, 576, 413
Zhekov, S.A. & Palla, F. 2004, *MNRAS*, 382, 1124
Zsargó, J., Hillier, D.J., Bouret, J.-C., Lanz, T., Leutenegger, M.A., Cohen, D.H., 2008, *ApJ*, 685, 149